Int J Biochem Mol Biol 2023;14(5):87-100
www.ijbmb.org /ISSN:2152-4114/IJBMB0151386

Original Article

Changes in phospholipid profiles in early larval stages of the marine mussel *Mytilus galloprovincialis* indicate a role of ceramides in bivalve development

Teresa Balbi[1,2*], Francesco Trenti[3*], Graziano Guella[3], Angelica Miglioli[4], Kristina Sepčić[5], Caterina Ciacci[6], Laura Canesi[1,2]

[1]Department of Earth, Environmental and Life Sciences (DISTAV), University of Genoa, Genoa, Italy; [2]NBFC, National Biodiversity Future Center, Palermo, Italy; [3]Bioorganic Chemistry Laboratory, Department of Physics, University of Trento, Trento, Italy; [4]Laboratoire de Biologie du Développement, Sorbonne Université/CNRS, Villefranche-sur-Mer, France; [5]Department of Biology, Biotechnical Faculty, University of Ljubljana, Ljubljana, Slovenia; [6]Department of Biomolecular Sciences, University "Carlo Bo" of Urbino, Urbino, Italy. [*]Equal contributors.

Received May 23, 2023; Accepted September 26, 2023; Epub October 15, 2023; Published October 30, 2023

Abstract: Background: Phospholipids are highly diverse molecules with pleiotropic biological roles, from membrane components and signaling molecules, whose composition can change in response to both endogenous and external stimuli. Recent lipidomic studies on edible bivalve mollusks were focused on lipid nutritional value and growth requirements. However, no data are available on phospholipid profiles during bivalve larval development. In the model marine bivalve *Mytilus galloprovincialis*, early larvae (up to 48 hours post fertilization-hpf) undergo dramatic molecular and functional changes, including shell biogenesis and neurogenesis, that are sustained by egg lipid reserves. Changes in phospholipid composition may also occur participating in the complex processes of early development. Objective: The lipidome of *M. galloprovincialis* eggs and early larval stages (24 and 48 hpf) was investigated in order to identify possible changes in phospholipid classes and related metabolic pathways that may play a role in key steps of development. Materials and methods: Lipidomic analysis were performed by NMR spectroscopy and liquid chromatography-mass spectrometry (LC-MS), with focus on phospholipids. Shifts in relative species composition of phosphatidylcholine, phosphatidylethanolamine, plasmalogen, and ceramide aminoethylphosphonate-CAEP, the bivalve analogue of the main mammalian ceramide sphingomyelin, were observed. Expression of genes involved in ceramide homeostasis was also modulated from eggs to early larval stages. Results: The results represent the first data on changes in phospholipid composition in bivalve larvae and suggest a functional role of phospholipids in mussel early development. Conclusion: The results underline the importance of lipidomic studies in bivalve larvae, in both physiological conditions and in response to environmental stress.

Keywords: Lipidome, bivalves, Mytilus, early development, phospholipids, ceramides

Introduction

Lipids are a broad class of highly diverse molecules with pleiotropic biological roles. They have been classified in fatty acids, glycerolipids, glycerophospholipids, sphingolipids, sterol lipids, prenol lipids, saccharolipids and polyketides, each including different classes and subclasses (https://www.lipidmaps.org). Different lipids are responsible for energy production and storage (i.e., triglycerides), represent the main structural components of cell membranes (i.e., phospholipids) and play key roles in cell signaling (i.e., phosphatidylinositols, diacylglycerol, phosphatidic acid, sphingosine-1-phosphate, ceramide-1-phosphate, eicosanoids) (https://www.lipidmaps.org/resources/lipidweb).

Since they are highly abundant and ubiquitous across all organisms, and their composition often changes drastically in response to external stimuli [1, 2], lipids represent a class of molecules with a unique promise for environmental science. Thanks to the development of analytical techniques, revealing the complexity

of the lipidome in a wide range of species living in different environments, environmental lipidomics represents an emerging concept in understanding the response of organisms and ecosystems to a changing world.

In marine invertebrates, although main lipid classes and fatty acids have been widely investigated, data on lipidomes are still limited to few species [3-6]. In edible bivalve mollusks (mussels, oysters, clams), lipidomics has been recently applied in studies on their nutritional value, and their requirements for growth [7-10]. This information is crucial for bivalve aquaculture in terms of traceability, shelf-life of the commercial product, physiology of reproduction, larval development, possible impact of contaminants and climate changes, and host-pathogen interactions.

Main lipid classes identified in bivalves include glycerophospholipids, sphingolipids, glycerolipids, fatty acids and sterols [7]. Among these, sphingolipids are a numerous and versatile group that are abundant in cellular membranes, characterized by a ceramide (e.g., 2-*N*-acyl-sphingosine) backbone. Sphingosine-based degradation products participate in many physiological processes, including signaling events that modulate multiple cellular functions (apoptosis, proliferation, differentiation, inflammation) [11, 12]. The diversity of biological roles of sphingolipids suggests their importance across a variety of organisms, life stages and environmental conditions.

Many invertebrates possess characteristic ceramides (e.g., ceramide phosphoethanolamine-CPE, ceramide aminoethylphosphonate-CAEP), that are analogues of vertebrate sphingomyelin [13]. In bivalves, CAEP often represents the third most abundant polar lipid after phosphatidylcholine (PC) and phosphatidylethanolamine (PE) [8, 11]. Recent lipidomic analyses of immune cells (hemocytes) of the marine bivalve *Mytilus galloprovincialis* revealed the presence of 29 mol% CAEP among all phospholipids [14], in line with data obtained by analyzing the whole adult and juvenile *Mytilus* spp. lipidome [7, 8, 15]. Ceramides may play different physiological roles in adult bivalves. For example, in the gills of oysters (*Crassostrea virginica*), changes in expression of ceramide-related genes induced by bacterial challenge suggested the role of ceramides in stress and/or immune responses [16]. In the hepatopancreas, two tightly associated enzymes, ceramide glycanase and ceramidase, were identified, that are responsible for generation of sphingosines and fatty acids to serve as signaling factors and energy source [17].

Embryos and larvae of marine species are particularly vulnerable to the stressors associated with ocean-related global changes [18]. Early larvae receive cellular defense mechanisms and energy reserves from eggs, that prepare them to face natural environmental variations; however, anthropogenic changes can affect these capacities [19]. Available data on lipid composition of bivalve eggs suggest that more than half of the energy requirements for embryogenesis is met by lipids, in particular by polyunsaturated fatty acids (PUFAs). These comprise 20:5(ω-3) (eicosapentaenoic acid-EPA), preferentially utilized as a source of energy, and 22:6(ω-3) (docosahexaenoic acid-DHA), as a structural compound, respectively [20]. However, information on the lipidome of early larval stages, in particular on phospholipids, is lacking. Membrane lipids modulate exchanges between the intracellular and the extracellular environment, and therefore play a key role in metabolic regulation and ion homeostasis [21]. Data on phospholipid composition may thus provide meaningful information to understand compositional changes in functional lipids across early developmental stages.

The mussel *Mytilus* spp. is a species of economic and ecological importance in coastal areas. In the Mediterranean mussel *M. galloprovincialis*, early larval stages (from the trocophora at 24 hpf to the first shelled D-veliger larva at 48 hpf) represent a critical point in development, when the blueprint for calcification and neurodevelopment are established [22-25]. Objective of the present work was to investigate the phospholipidome of early larval stages of *M. galloprovincialis*, in order to identify possible changes in phospholipid classes and related metabolic pathways that may play a role in key steps of development.

Data are presented on the lipidome of mussel eggs and early larval stages (24 and 48 hpf), with focus on membrane phospholipids, ceramides in particular. Lipidomic analyses were carried out by nuclear magnetic resonance spectroscopy (NMR) and liquid chromatography

coupled to mass spectrometry (LC-MS). Basal expression of genes involved in ceramide biosynthesis (serine palmitoyltransferase-1, 3-ketodihydrosphingosine reductase), metabolism (ceramide glucosyltransferase), and breakdown (acid ceramidase), was also evaluated by qPCR.

Methods

Mussels and larval development

Mussels (*M. galloprovincialis* Lam.), were purchased in February 2022 from an aquaculture farm in the Ligurian Sea (La Spezia, Italy) and acclimatized in static tanks containing aerated artificial sea water (ASW), pH 7.9-8.1, 36 ppt salinity (1 L/animal), 16±1°C, for 3 days. Gamete collection obtained by spontaneous spawning and fertilization were performed following [26]. After checking egg quality and sperm motility, fertilization was carried out with an egg:sperm ratio of 1:10 and fertilization success (n. fertilized eggs/n. total eggs ×100) was verified after 30 min by microscopic observation (>90%).

For lipid analysis, unfertilized eggs (about 3,000,000/sample) were centrifuged at 800× *g* for 10 min, at room temperature. Larvae were grown in 1 L of aerated ASW (200 larvae/mL), at 16±1°C, and collected at 24 and 48 hpf by centrifugation at 800× *g* for 10 min.

For qPCR analysis, unfertilized eggs (about 24,000 eggs/mL) were collected by centrifugation at 400× *g* for 10 min, at 4°C. Larvae grown in polystyrene 6-well plates (final volume 8 mL) were collected at 24 and 48 hpf by a nylon mesh (20 μm pore-filter), washed with ASW and centrifuged at 800 ×*g* for 10 min at 4°C [26]. For each larval stage, about 7,000 embryos/replicate were utilized. Larval pellets and unfertilized eggs were lysed in 1 mL of TRI Reagent (Sigma Aldrich, Italy) and stored at -80°C.

Larval samples were obtained from 3 or 4 independent parental pairs, respectively, for lipid and qPCR analysis.

Lipid extraction

Lipids were extracted from eggs and 24 and 48 hpf larvae following [27]. After sample collection by centrifugation, the pellets were re-suspended in 700 μL of milliQ water, then added with 3 mL of chloroform/methanol (2:1 v/v). Samples were sonicated in ice with a Tip Sonicator (UP200S Hielscher Ultrasonic Technology, Germany) for 20 min, at 100 W, with a 50% on/off cycle. The obtained suspension was vortexed thoroughly and centrifuged at 6000× *g* for 10 min at 4°C to separate the two phases. The lower phase was collected, and the inter-layer sediment and the aqueous phase were extracted again as described above. The lower phases, containing lipids, were dried by N_2 flux, weighted and stored at -80°C. Lipids were dissolved in 600 μL deuterated methanol (MeOH-d_4) for lipidomic analysis, as previously described in hemocytes of adult mussels [14].

Lipidomics

Lipidomic analyses were performed as previously described [14, 28].

Nuclear magnetic resonance analysis: ^{1}H-NMR (400 MHz) and ^{31}P-NMR (162 MHz) spectra of lipid extracts in MeOH-d_4 were recorded at 300 K by a nuclear magnetic resonance (NMR) spectrometer (400 MHz; Bruker-Avance, Bremen, Germany), with a 5-mm double resonance broadband observe probe and pulsed-gradient field utility. The ^{1}H-90° proton pulse length was 9.3 μs, with a transmission power of 0 db. The ^{31}P-90° proton pulse length was 17 μs, with a transmission power of -3 db. The probe temperature was maintained at 300.0 K (±0.1 K) using a variable temperature unit (B-VT 1000; Bruker). Calibration of the chemical shift scale (δ) was performed on the residual proton signal of the MeOH-d_4 at δ_H 3.310, and the phosphatidylcholine (PC) signal at δ_P -0.550 ppm was used for calibration of the ^{31}P-NMR δ scale. The following measurements were performed: ^{1}H-NMR (i.e., proton chemical shifts, scalar couplings) and ^{31}P-NMR composite pulse decoupling in order to remove any proton coupling in ^{31}P-NMR spectra, where generally 4000 free induction decays were acquired and processed using exponential line broadening of 0.3 Hz prior to Fourier transformation. The resulting one-dimensional NMR (1D-NMR) spectra were analysed using TopSpin 3.6.1 (Bruker, Bremen, Germany). The lipid classes from NMR data

were identified through comparisons to available lipid standards.

HPLC-electrospray ionization-mass spectrometry analysis: Lipid extract were analysed by liquid chromatography-mass spectrometry (LC-MS) (Model 1100 series; Hewlett-Packard) coupled to a quadrupole ion-trap mass spectrometer (Esquire LCTM; Bruker, Bremen, Germany) equipped with an electrospray ionisation source in both positive and negative ion modes [28]. Chromatographic separation of lipids was carried out at 303 K on a thermostatted C18 column (Kinetex 2.6 μ; length, 100 mm; particle size, 2.6 μm; internal diameter, 2.1 mm; pore size, 100 Å; Phenomenex, Torrence, CA, USA). The solvent system consisted of eluent A as MeOH/H_2O (7:3, v/v) containing 10 mM ammonium acetate, and eluent B as isopropanol/MeOH (10:90, v/v) containing 10 mM ammonium acetate. Samples were resuspended in 1 mL $CHCl_3$/MeOH (2:1, v/v), and aliquots of 10 μL were run with a linear gradient of eluent B from 65% to 100% for 40 min, followed by 20 min isocratic elution with 100% B at 1 mL/min, to elute the diglycerides and triglycerides. The column was then equilibrated with 65% B for 10 min. The MS scan range was 50-1500 m/z, at 13,000 U/s, with a mass accuracy of ~100 ppm. The nebuliser gas was high purity nitrogen at a pressure of from 20 to 30 psi, a flow rate of 6 L/min and at 300°C. The electrospray ionisation was operated in positive ion mode for the qualitative analyses of triglycerides (TAG), phosphatidylcholine (PC), plasmenyl-PC (pPC), and sphingomyelin (SM). Both positive and negative ion modes were set for phosphatidylinositol (PI), phosphatidylethanolamine (PE), plasmenyl-PE (pPE) and CAEP, while negative mode was implemented for free fatty acids (FFAs). Data are reported as relative abundance with a 1% cutoff.

Lipidomic data analysis: NMR and MS data were analyzed as previously described [14, 28]. ^{1}H-NMR data were processed to evaluate the molar ratio of all lipids, including phospholipids, triglycerides (TAGs), and sterols. ^{1}H-NMR data were also utilized to calculate the content of polyunsaturated (PUFA), monounsaturated (MUFA), and saturated acyl chains (SFA). Peaks were normalized by the number of protons corresponding to each signal. In order to calculate the PUFA, MUFA and SFA molar fractions, the ^{1}H-NMR signal corresponding to the α-protons (2.30 ppm) was normalized to 100%, as all lipids contribute to this signal. ^{31}P-NMR data were analyzed to evaluate the molar fractions of different phospholipid classes. Molar fractions were calculated by integrating all ^{31}P-NMR signals relative to the sum of total phospholipids in the sample (normalized to 100%). The integral of a single ^{31}P-NMR signal (relative to each phospholipid class) was divided by the sum of all integrals, hence giving its molar fraction as a percent value. The results represent the percentage of each class with respect to total phospholipids. LC-MS data were utilized to evaluate the lipid distribution within each class. As different lipid classes have different ionization response in ESI LC-MS, the molar fraction of members of each class was calculated by integrating the MS peaks of all lipids and normalizing to 100% the sum of all integrals of the lipids of the same class. Each percentage was then calculated by dividing the integral of each lipid species against the sum of all integrals within the same class.

qPCR

Selected gene sequences were identified by Blastp and Blastx in the reference genome of *M. galloprovincialis* [29] using previously published bivalve sequences as main reference [16]. Open reading frames (ORF) for each gene were identified with Expasy Translate Tool (https://web.expasy.org/translate/). Selective primer pairs for each gene were designed with NCBI Primer Blast (https://www.ncbi.nlm.nih.gov/tools/primer-blast/) (Table S1). All procedures (RNA extraction, retro-transcription and qPCR) were carried out as in [26]. Briefly, after extraction, RNA concentration and quality were verified using the Qubit RNA assay (ThermoFisher, Milan, Italy) and electrophoresis using a 1.5% agarose gel under denaturing conditions. Aliquots of 1 μg RNA were reverse-transcribed into cDNA [26]. qPCR reactions were performed in triplicate in a final volume of 15 μL in a CFX96™ Real-Time qPCR system apparatus (Biorad, Milan, Italy) using a standard "fast mode" thermal protocol (60°C). Details on qPCR conditions are reported in Table S1. A control lacking cDNA template (no-template) was included. Expression of target mRNAs was calculated by a comparative C_T

method using HEL and EF-α1 as reference genes [26]. Data are reported as relative expression in larvae (log_2-transformed fold changes) with respect to eggs.

Statistics

Data on phospholipid composition were analysed by two-way ANOVA followed by the Bonferroni's post-test (P≤0.05) using GraphPad Prism 6 software (GraphPad Inc.). Multivariate statistical analyses, including heat map clustering, principal component analysis (PCA) and partial least squares-discriminant analysis (PLS-DA) were performed using MetaboAnalyst 5.0 (https://www.metaboanalyst.ca) [30]. For qPCR, data were analysed using the non-parametric one-way ANOVA followed by the Mann-Whitney *U* test (P≤0.05), using GraphPad Prism 6 software (GraphPad Inc.).

Results

Total lipids

^{1}H-NMR analysis of lipid extracts showed that in all groups (eggs, 24 and 48 hpf larvae) lipids containing PUFAs with ω-3 chains represented the most abundant class, followed by non ω-3 lipids, and by low amounts of sterols (cholesterol). Representative ^{1}H-NMR spectra of each group are shown in Figure S1A-C. The proportion of non ω-3 lipids progressively increased from eggs to 48 hpf larvae (from 66 to 87% of the total), whereas an opposite trend was observed for ω-3 lipids (from 32 to 12%). Also, the amount of sterol was higher in eggs with respect to larvae (2 and 1%, respectively) (Figure S1D).

Phospholipids

The relative molar fractions of phospholipid classes were determined through the ^{31}P-NMR spectra as previously described [14]. As shown in **Figure 1**, PC+pPC represented the majority of phospholipids in all samples (with an average molar distribution ≈53%), followed by pPE (≈36%) and CAEP (≈11%), showing a similar proportion in eggs and larvae. No PE and PI were identified by ^{31}P-NMR.

Characterization of lipid species

The overall profile of TAG, FFA, and phospholipids, in terms of chain lengths and unsaturation, was evaluated by LC-MS.

Total TAGs and FAAs: Among TAGs, 38 species were identified in all samples (Figure S2), with a total number of carbons (from 48 to 58) and a high degree of unsaturation (average 6 C=C bonds). The most abundant TAGs were 52:6, 54:6 and 56:10. Relative TAG composition did not significantly change among eggs and larval stages (Figure S2). Nine main FFAs were identified in eggs, 24 and 48 hpf larvae (**Figure 2**). In all samples, the major class was represented by saturated FAAs (SFA) (with the molar sum of 14:0, 16:0 and 18:0 representing from 71% of total FFAs in eggs to 84% in 48 hpf larvae), followed by PUFAs (from 27 to 12%) and by a lower amount of monounsaturated FAs (MUFA) (from 2 to 4%) (**Figure 2A**). Changes in relative amounts of different FFAs were observed across development; interestingly, a large and significant decrease in ω-FAA 20:5 (EPA) was observed in 48 hpf larvae with respect to eggs (about -50%) (**Figure 2B**).

Phospholipids: In all samples, up to 56 phospholipid species among PC, PE, PI and CAEP were identified. The heatmaps obtained from 3 independent parental pairs (Samples 1, 2 and 3) (**Figure 3**) show a similar trend in composition of different phospholipids from eggs to 24 and 48 hpf larvae in all samples. Samples 1 and 3 were homogeneous, whereas Sample 2 showed generally higher values for all phospholipid species at each developmental stage. Overall, the relative amounts of different phospholipid show evident dynamic changes from eggs to 24 and 48 hpf larvae.

A Principal Component Analysis (PCA) was first applied to all samples. Figure S3 shows the scores plot (PC2 *vs* PC1), with PC1 explaining 60% of total variance, indicating only a partial separation among eggs, 24 and 48 hpf larvae. A better separation could be observed when considering PC2 and PC3, that together explain about 30% of total variance.

Partial Least Squares-Discriminant Analysis (PLS-DA) was subsequently applied for the classification of eggs, 24 and 48 hpf larvae, and the results are reported in **Figure 4**. As shown in **Figure 4A**, each group was clearly separated, indicating distinct phospholipid profiles among different groups of samples, with components 1 and 2 explaining, respectively, 37.3% and 37.6% of the total variance. **Figure 4B** reports the VIP (Variable Importance in Projection) score plot of the top 15 phospholipid species

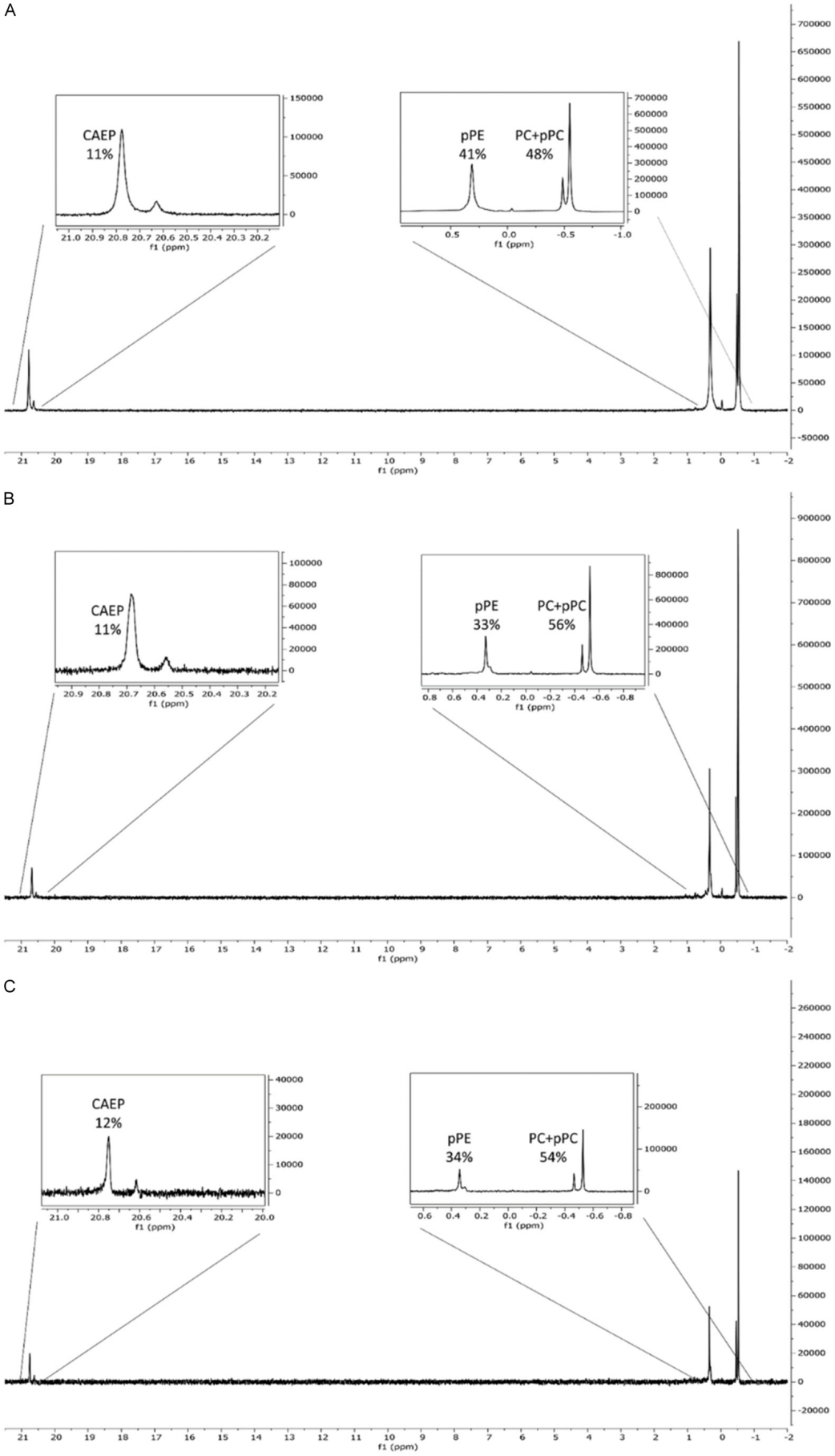
A
CAEP
11%
pPE
41%
PC+pPC
48%
f1 (ppm)
B
CAEP
11%
pPE
33%
PC+pPC
56%
f1 (ppm)
C
CAEP
12%
pPE
34%
PC+pPC
54%
f1 (ppm)

Figure 1. ^{31}P-NMR spectra of phospholipid classes in lipid extracts from *M. galloprovincialis* eggs (A) and larvae at 24 (B) and 48 (C) hpf. CAEP = ceramide aminoethylphosphonate; pPE = plasmenyl phosphatidylethanolamine; PC = phosphatidylcholine; pPC = plasmenyl-PC. The molar fraction of each class was calculated by signal integration and expressed as percentage of total phospholipids.

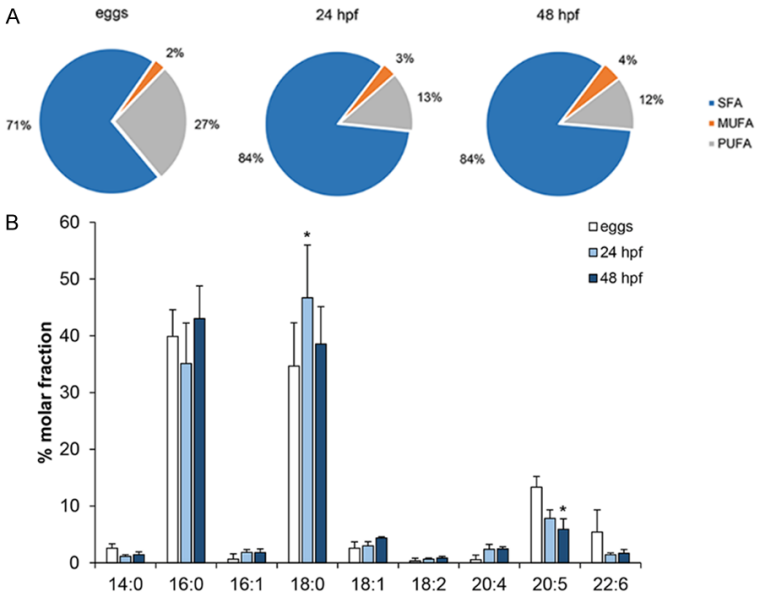

Figure 2. LC-MS analysis of main free fatty acids (FFAs) in total lipid extracts from *M. galloprovincialis* eggs and larvae at 24 and 48 hpf. A. Relative composition (%) in main FFAs: SFA = saturated FA; MUFA = monounsaturated FA; PUFA = polyunsaturated FA; B. FFA species. Data, representing the mean ± stdev of 3 samples, are expressed as % molar ratio of total FFAs. Significant differences with respect to eggs are reported (* = P≤0.05, Two-way ANOVA, Bonferroni post-test).

selected based on the PLS-DA model for Component 1. The phospholipid species that contributed mostly to the discrimination, with recorded VIP values exceeding 1.5 [31], were PC 36:6II, PPE 18:1/22:2, PPE 38:5II, CAEP 34:1 and PPE 18:1/20:1.

Quantitative changes in phospholipids across development: Quantitative changes in relative composition of different phospholipid species in each class were evaluated.

Twenty PC species were identified in all samples (Figure S4), including a mixture of canonical PC (80%) and pPC (about 20%). The most abundant PCs were 36:5 (≥25%), 38:6 (≥12%), and pPC 36:5 (≥10%). At 48 hpf, significant decreases were observed in the amount of PC 36:5, and increases in PC 38:6, respectively, in comparison to eggs and 24 hpf larvae. Seventeen PE species were identified, all represented by pPE (Figure S5). The most abundant were pPE 18:1/20:5 (≥30%) and 18:1/20:2 (≥10%). At 48 hpf, significant decreases were observed for pPE 18:1/20:5 and 20:2/20:5, whereas the amount of pPE 18:1/20:2, 18:1/22:2 and 40:4 was higher with respect to eggs and 24 hpf larvae.

LC-MS allowed for identification and quantification of 4 PI species (38:4, 38:5, 40:5 and 40:6). At 48 hpf, a significant increase was observed for PI 40:5 with respect to eggs and 24 hpf larvae (Figure S6). Finally, fifteen different CAEP were identified in all samples (**Figure 5**). The most abundant CAEP were 35:3 diene (≥32%), 34:3 diene (≥22%), 34:2 (≥13%) and 35:3 Met (≥5%). A progressive decrease in CAEP 34:2 and increase in CAEP 35:3 diene, respectively, were observed throughout development.

Expression of ceramide-related genes across early development

Expression of genes involved in ceramide biosynthesis (SP2, KDSR2), metabolism (GC2), and degradation (aCDase), was evaluated in 24 and 48 hpf larvae compared with eggs. The results (**Figure 6**) indicate that SP2, the rate-limiting enzyme in sphingolipid synthesis, is highly upregulated with respect to eggs from 24 hpf (up to 100-fold at both 24 and 48 hpf, P≤0.05). Increased expression of KDSR2, that catalyzes the reduction of 3-ketodihydrosphingosine to dihydrosphingosine, was also observed (+60% at 24 hpf *vs* eggs, P≤0.05). In contrast, GC2, involved in ceramide glycosylation to form glucosylceramide, the core structure of many glycosphingolipids, was significantly downregulated at 48 hpf with respect to eggs and to 24 hpf larvae (-55%, P≤0.05). Also aCDase, that hydrolyzes lysosomal membrane ceramide into sphingosine, the backbone of all sphingolipids [32], was progressively upregu-

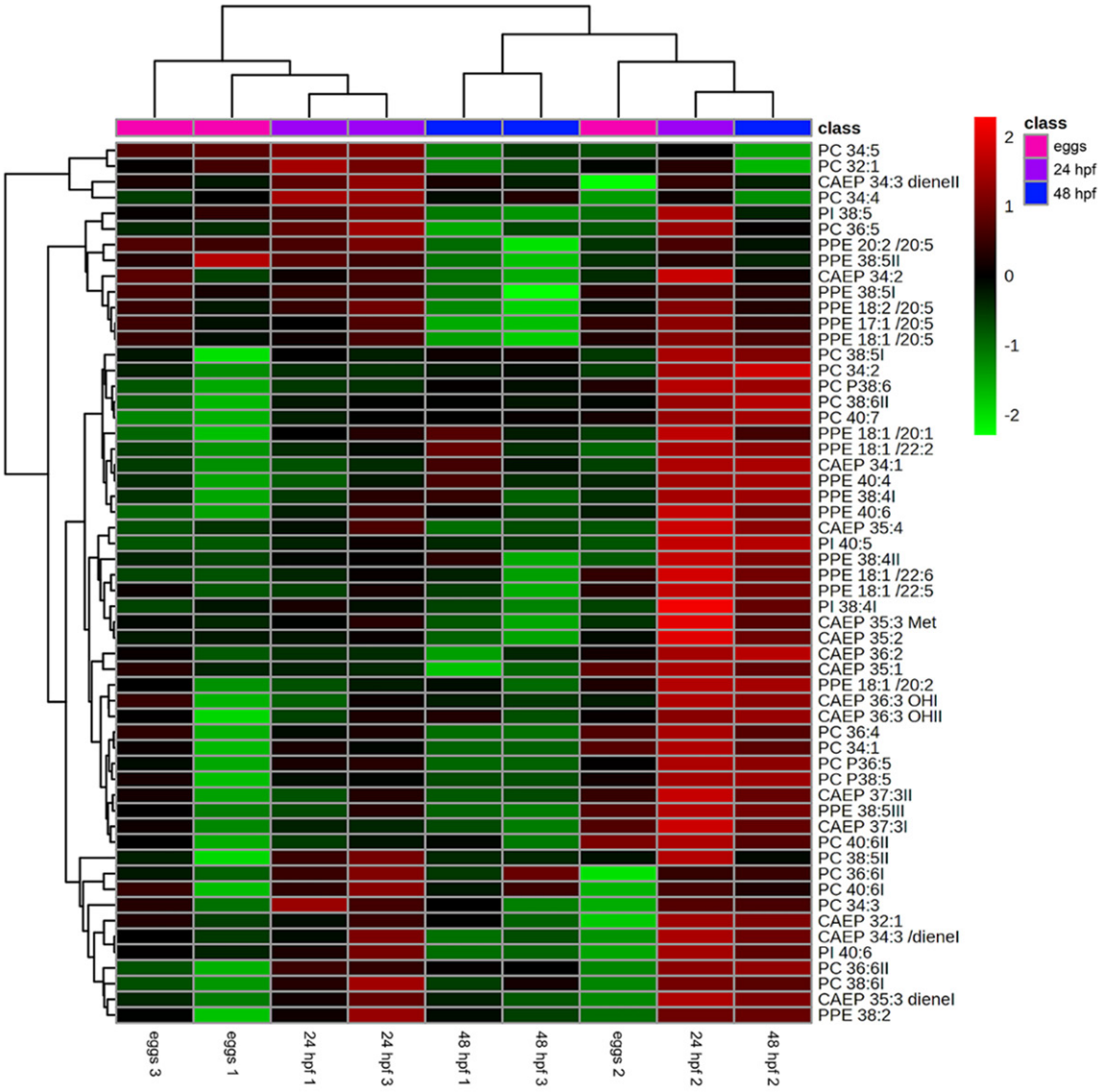

Figure 3. Heatmap showing the relative amounts of phospholipids in *M. galloprovincialis* eggs, 24 and 48 hpf larvae. The results are the mean of 3 samples obtained from independent parental pairs (eggs 1, eggs 2, eggs 3; 24 hpf 1, 24 hpf 2, 24 hpf 3; 48 hpf 1, 48 hpf 2, 48 hpf 3).

lated across development (up to 4,5-fold at 48 hpf, P≤0.05).

Discussion

The results obtained represent the first lipidomic data in early development of *M. galloprovincialis*, one of the main economically and ecologically relevant species of bivalves worldwide. The lipid profile of mussel eggs and first larval stages (24 and 48 hpf) was characterized through untargeted lipidomic analysis using NMR spectroscopy and LC-MS, as previously described in hemocytes of adult mussels [14].

The results of ^{1}H-NMR analysis indicated a decrease in ω-3 containing lipids from eggs to larvae. Such a change most likely reflects the oxidative degradation of PUFAs as a source of energy in early developmental stages, where larvae were not fed. This highlights the role of energy-supply by ω-3 PUFAs in molluscan embryogenesis as previously reported ([33] and refs. therein). The decrease in PUFAs observed in both 24 and 48 hpf larvae with

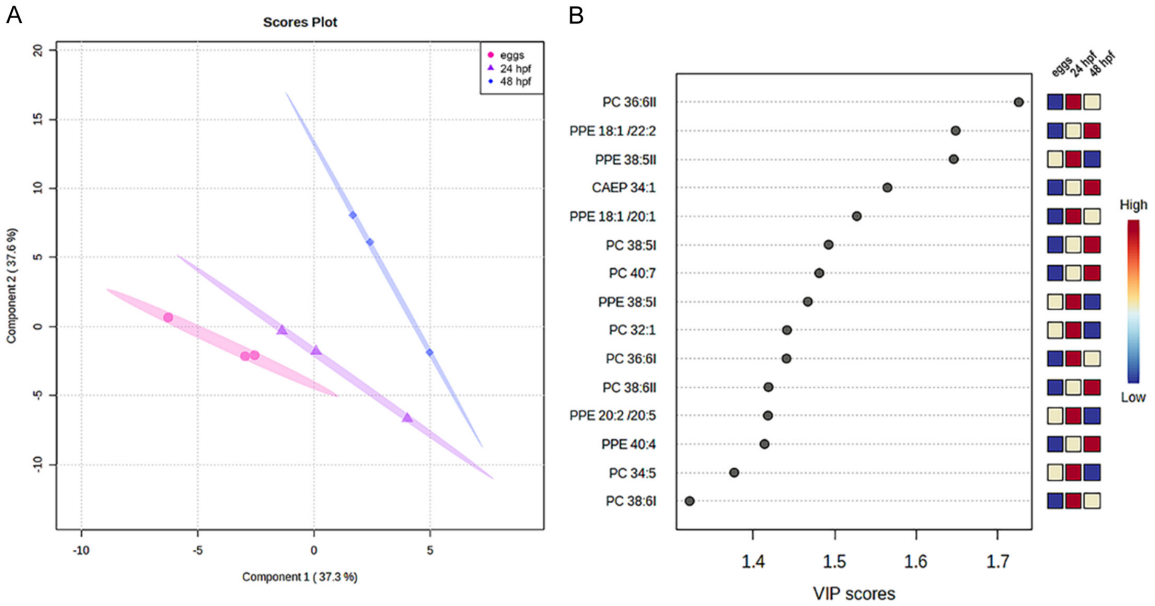

Figure 4. PLS-DA score plots of phospholipid data (PC, PE, PI, CAEP species) in eggs, 24 and 48 hpf larvae. The explained variances are shown in brackets. A. 2D plot of Components 1 and 2. The colored ellipses represents the 95% confidence interval; the explained variations are shown in brackets. B. Top 15 phospholipids with the highest VIP scores at three different developmental stages; the colored boxes indicate the relative concentrations of the corresponding lipid species in each group.

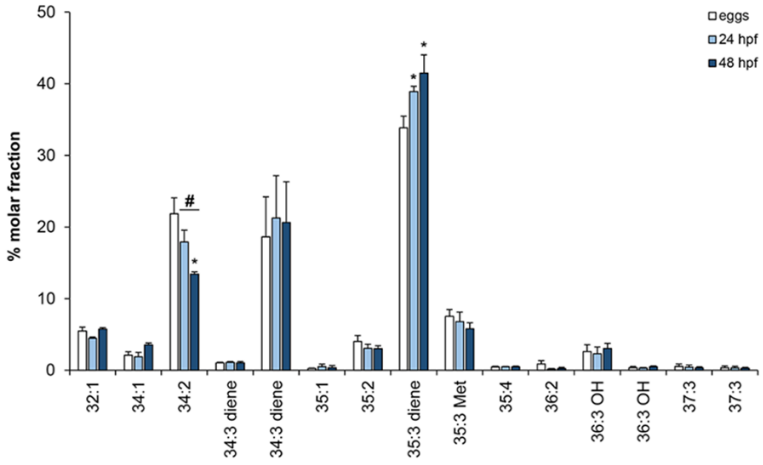

Figure 5. LC-MS analysis of main CAEP species in lipid extracts from *M. galloprovincialis* eggs and larvae at 24 and 48 hpf. Data, representing the mean ± stdev of 3 samples, are expressed as % molar ratio of total CAEP. Significant differences (* eggs *vs* 24 or 48 hpf; # 24 *vs* 48 hpf; P≤0.05, Two-way ANOVA, Bonferroni post-test) are reported.

respect to eggs could be partly ascribed to 20:5 (EPA), as subsequently indicated by FFA analysis by LC-MS. These FFAs, together with 22:6 PUFAs, are of particular importance in membrane integrity, as structural modulators of enzymes, transporters and receptors, and as precursor of signaling molecules, thus regulating multiple cellular functions [20]. Our data are in line with those obtained in the first larval stages of the scallop *Pecten maximus*, where a decrease in the amount of 20-carbon PUFAs was observed, reflecting a metabolic activity specific to this lipid class in the early endotrophic phase of development, when larvae only rely on maternal lipids [34].

^{31}P-NMR analysis identified 3 main phospholipid classes (PC, PE and CAEP), with a similar proportion of PC (50%) > PE (40%) > CAEP (13%) in both eggs and larvae. Their relative content was different from that recently described in the hemocytes of adult specimens of *M. galloprovincialis* [14], with PC (36%) > PE (35%) > CAEP (29%), in line with literature data on adult tissues of this species [13, 15].

LC-MS was also utilized to identify phospholipid species. The results indicate dynamic changes

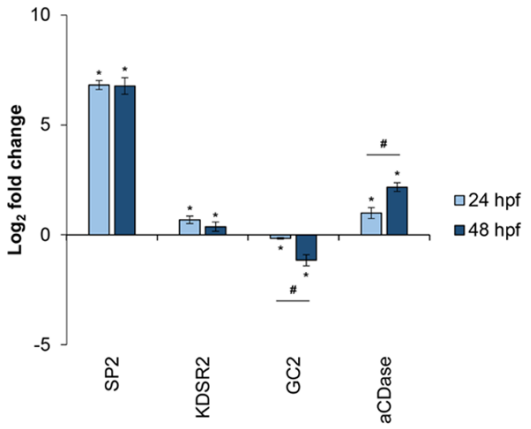

Figure 6. Basal expression of genes involved in ceramide metabolism in *M. galloprovincialis* larvae at 24 hpf and 48 hpf larval stages. SP2 = serine palmitoyltransferase-1; KDSR2 = 1,3-ketodihydrosphingosine reductase; GC2 = ceramide glucosyltransferase; aCDase = acid ceramidase. Data (mean ± stdev) are reported as relative expression (log_2-transformed fold changes) with respect to eggs. * eggs *vs* 24 or 48 hpf, P≤0.05; # 24 hpf *vs* 48 hpf, P≤0.05.

in relative composition of phospholipids across early larval development. PLS-DA analysis showed a clear separation among eggs, 24 and 48 hpf larvae, indicating that each group is characterized by a distinct phospholipid profile; moreover, the obtained VIP scores identified PC 36:6II, pPE 18:1/22:2, pPE 38:5II, CAEP 34:1 and pPE 18:1/20:1 as those phospholipids that contribute mostly to the discrimination among the three groups.

Quantitative analysis of different species in each phospholipid class revealed changes in relative composition of PC and PE, in particular of pPC and pPE. Shellfish are rich in polar lipids, especially glycerophospholipids, such as plasmalogens, characterized by a vinyl ether bond at *sn*-1 position and an ester bond at *sn*-2 position: these phospholipids play critical roles in cellular membrane structure-mediated functions and in membrane protein activity, also acting as a storage pool of long chain PUFAs, EPA and DHA in particular ([12] and refs. therein). A study on six species of adult bivalves showed that the mussel *Mytilus edulis* has the highest percentage of plasmalogens [12]. In the present work, 20 plasmalogen species were identified in eggs and larvae of *M. galloprovincialis,* 17 of which represented by pPE, all unsaturated, containing up to seven double bonds. The composition and relative amounts of different PC, pPC, and pPE in eggs and larval samples was distinct from that observed in cells of adult mussels evaluated with the same techniques [14], since eggs and larvae showed higher amounts of pPC, lower amounts of pPE and only traces of PE (<1%, not shown) compared with hemocytes. Interestingly, 48 hpf larvae showed significant changes in the amount of different pPC and pPE, suggesting specific roles of plasmalogens in the larval transition to the first D-shell stage.

With regards to CAEP, the results represent the first data on their identification in eggs and first larval stages of marine invertebrates, and confirm that CAEP is the third most abundant phospholipid in bivalves, after PC and PE. However, the total CAEP content was lower in eggs and larvae (13%) than in tissues and cells of adult and juvenile mussels (about 30%) [7, 8, 14]. Moreover, eggs and larvae were characterized by the presence of CAEP dienes and the absence of hydroxylated CAEPs (CAEP 35:3OH) compared with hemocytes [14]. What is more, our data show that the relative amounts of different CAEP species, and in particular that of the most abundant CAEP (34:2 and 35:3 diene) are progressively modified from eggs to both larval stages, suggesting a role for ceramide-based polar lipids across early development.

A recent detailed lipidomic study on larval development of marine mollusks was performed on the gastropod *Haliotis discus hannai* [31]. The results showed alterations in the composition of TAGs and different phospholipids at later developmental stages (96 h and 90 days old larvae) with respect to the present study. In *Mytilus* early development, the transition from 24 hpf (first trocophora stage) to the first shelled larva, the D-veliger stage, within the first 48 hpf, is probably the most dramatic event to occur [22, 35, 36]. Such a transition involves profound molecular and functional modifications leading to first neurodevelopment, shell biogenesis, and organogenesis. These modifications must rely on a complex regulation of differentiation, proliferation and apoptotic processes, that will utilize lipids not only as an endogenous energy source, but also as signaling molecules. During the transition to the first D-veliger stage of *C. gigas*, transcriptomic and metabolomics data underlined

changes in phospholipid metabolic processes [36]. However, compared to other-omics approaches, lipidomics has not been so far applied in early bivalve development [37].

The results here obtained suggest that phospholipids may play multiple functional and structural roles in bivalve first developmental stages; among these, CAEP is a bivalve-specific ceramide-based lipid similar to sphingomyelin, which plays key structural and functional roles in vertebrate cell membranes [7, 8, 13, 16]. Although the amount of total CAEP did not change across early mussel development, the results indicate a rearrangement in relative amounts of different CAEP species from eggs to early larval stages, suggesting changes in ceramide-based metabolism.

Ceramide is an important lipid cell-signaling factor that, beside acting as a precursor for all complex sphingolipids, is involved in numerous effector pathways, e.g. in kinase-mediated transduction cascades and different downstream responses [11]. Ceramides regulate apoptosis and cell differentiation, two processes at the core of embryo development [38], in both mammals and in the zebrafish [39, 40]. Transcriptomic analysis in the clam *Venerupis decussata* revealed changes in genes related to the regulation of ceramide levels during oocyte maturation [41]. Changes in ceramide metabolism may thus play a physiological role also in early bivalve development.

All *de novo* ceramide synthesis starts with the condensation of L-serine with palmitoyl-coenzyme A, catalyzed by serinepalmitoyl transferase (SP), and it produces 3-ketosphinganine, which can be further reduced to dihydrosphingosine by 3-ketoreductase [11]. In order to shed some light on ceramide metabolism, expression of four genes that represent key steps in ceramide metabolism was evaluated; these genes were selected in *Mytilus* genome in analogy with those previously identified in *C. gigas* [16]. The results indicate significant changes in the expression pattern of all genes across early development. In particular, a strong upregulation of SP2, the rate-limiting enzyme in sphingolipid synthesis, was observed from 24 hpf with respect to eggs, indicating increased biosynthesis of ceramides during early larval stages. Downregulation of GC2, that participates in the initial step of the glucosylceramide-based synthetic pathway, would further contribute to increase ceramide levels. On the other hand, a progressive upregulation of aCDase, that catalyzes the hydrolysis of ceramide into sphingosine and FFA, was also observed, in line with reports showing that this enzyme is required for early embryo survival [42]. Increased ceramide production (through *de* novo synthesis or reduced metabolism via glycosylation) may be necessary to stimulate the signaling pathways necessary for early developmental processes. In larvae at 24 hpf, differentiation of first neurons occurs, accompanied by upregulation of components of the serotonergic and dopaminergic system [23-25]. Since ceramide is a modulator of monoamine transporter function [43], its levels may regulate early neurodevelopment [23-25]. However, ceramide accumulation may be followed by increased metabolism after it has performed its signaling roles. Moreover, its metabolite sphingosine/sphingosine 1-phosphate may function as a downstream signaling molecule in regulating cell growth, proliferation, differentiation, and survival [17].

Conclusion

Overall, the results indicate that changes in phospholipid profiles may reflect the functional roles of these lipids in early mussel development. These data can represent the basis for future research of the lipidome of marine bivalves in development and growth in healthy, stressed and pathologic conditions. With regards to ceramides, they are involved in the progression of several human diseases, and are thus utilized as biomarkers of heart and metabolic dysfunctions [44, 45]. Information on ceramide levels and composition in bivalve larvae and adults may open up the possibility to utilize these lipids as health biomarkers also in marine bivalves. This is of utmost importance when considering that bivalve populations, that represent key ecological components in coastal ecosystems and include economically important aquacultured species, have been subjected to a significant decline in the last two decades [46, 47]. Such a decline is due to multiple causes, including the impact of changing climate conditions [48]. The sensitivity of larval stages to environmental perturbations, including predicted changes in ocean temperature and pH, may represent a key fac-

tor. Future research on changes of phospholipid-related biomarkers in bivalves in response to environmental changes would be of importance in a global change scenario.

Acknowledgements

The authors wish to thank Dr. Michele Montagna for his invaluable technical assistance. This research was partly supported by Fondi di Ricerca di Ateneo - University of Genoa (FRA2020), and Slovenian Research Agency (N° P1-0207).

Disclosure of conflict of interest

None.

Address correspondence to: Teresa Balbi, Department of Earth, Environmental and Life Sciences (DISTAV), University of Genoa, Corso Europa 26, 16132 Genova, Italy. ORCID: 0000-0002-7495-6000; E-mail: Teresa.Balbi@unige.it

References

[1] Koelmel JP, Napolitano MP, Ulmer CZ, Vasiliou V, Garrett TJ, Yost RA, Prasad MNV, Godri Pollitt KJ and Bowden JA. Environmental lipidomics: understanding the response of organisms and ecosystems to a changing world. Metabolomics 2020; 16: 56.

[2] Lutier M, Di Poi C, Gazeau F, Appolis A, Le Luyer J and Pernet F. Revisiting tolerance to ocean acidification: insights from a new framework combining physiological and molecular tipping points of Pacific oyster. Glob Chang Biol 2022; 28: 3333-3348.

[3] Lee MC, Park JC and Lee JS. Effects of environmental stressors on lipid metabolism in aquatic invertebrates. Aquat Toxicol 2018; 200: 83-92.

[4] Imbs AB, Ermolenko EV, Grigorchuk VP, Sikorskaya TV and Velansky PV. Current progress in lipidomics of marine invertebrates. Mar Drugs 2021; 19: 660.

[5] Chen E, Kiebish MA, McDaniel J, Gao F, Narain NR, Sarangarajan R, Kacso G, Ravasz D, Seyfried TN, Adam-Vizi V and Chinopoulos C. The total and mitochondrial lipidome of Artemia franciscana encysted embryos. Biochim Biophys Acta 2016; 1861: 1727-1735.

[6] Rey F, Cartaxana P, Aveiro S, Greenacre M, Melo T, Domingues P, Domingues MR and Cruz S. Light modulates the lipidome of the photosynthetic sea slug Elysia timida. Biochim Biophys Acta Mol Cell Biol Lipids 2023; 1868: 159249.

[7] Laudicella VA, Whitfield PD, Carboni S, Doherty MK and Hughes AD. Application of lipidomics in bivalve aquaculture, a review. Review in Aquaculture 2020; 12: 678-702.

[8] Laudicella VA, Beveridge C, Carboni S, Franco SC, Doherty MK, Long N, Mitchell E, Stanley MS, Whitfield PD and Hughes AD. Lipidomics analysis of juveniles' blue mussels (Mytilus edulis L. 1758), a key economic and ecological species. PLoS One 2020; 15: e0223031.

[9] Li H, Song Y, Zhang H, Wang X, Cong P, Xu J and Xue C. Comparative lipid profile of four edible shellfishes by UPLC-Triple TOF-MS/MS. Food Chem 2020; 310: 125947.

[10] Liu Z, Zhao M, Wang X, Li C, Liu Z, Shen X and Zhou D. Investigation of oyster Crassostrea gigas lipid profile from three sea areas of China based on non-targeted lipidomics for their geographic region traceability. Food Chem 2022; 386: 132748.

[11] Panevska A, Skočaj M, Križaj I, Maček P and Sepčić K. Ceramide phosphoethanolamine, an enigmatic cellular membrane sphingolipid. Biochim Biophys Acta Biomembr 2019; 1861: 1284-1292.

[12] Wang J, Liao J, Wang H, Zhu X, Li L, Lu W, Song G and Shen Q. Quantitative and comparative study of plasmalogen molecular species in six edible shellfishes by hydrophilic interaction chromatography mass spectrometry. Food Chem 2021; 334: 127558.

[13] Facchini L, Losito I, Cataldi TR and Palmisano F. Ceramide lipids in alive and thermally stressed mussels: an investigation by hydrophilic interaction liquid chromatography-electrospray ionization Fourier transform mass spectrometry. J Mass Spectrom 2016; 51: 768-781.

[14] Balbi T, Trenti F, Panevska A, Bajc G, Guella G, Ciacci C, Canonico B, Canesi L and Sepčić K. Ceramide aminoethylphosphonate as a new molecular target for pore-forming aegerolysin-based protein complexes. Front Mol Biosci 2022; 9: 902706.

[15] Donato P, Micalizzi G, Oteri M, Rigano F, Sciarrone D, Dugo P and Mondello L. Comprehensive lipid profiling in the Mediterranean mussel (Mytilus galloprovincialis) using hyphenated and multidimensional chromatography techniques coupled to mass spectrometry detection. Anal Bioanal Chem 2018; 410: 3297-3313.

[16] Timmins-Schiffman E and Roberts S. Characterization of genes involved in ceramide metabolism in the Pacific oyster (Crassostrea gigas). BMC Res Notes 2012; 5: 502.

[17] Pavlova NV, Li SC and Li YT. Degradation of glycosphingolipids in oyster: ceramide glycanase and ceramidase in the hepatopancreas of oys-

ter, Crassostrea virginica. Glycoconj J 2018; 35: 77-86.
[18] Przeslawski R, Byrne M and Mellin C. A review and meta-analysis of the effects of multiple abiotic stressors on marine embryos and larvae. Glob Chang Biol 2015; 21: 2122-2140.
[19] Hamdoun A and Epel D. Embryo stability and vulnerability in an always changing world. Proc Natl Acad Sci U S A 2007; 104: 1745-1750.
[20] Hendriks IE, van Duren LA and Herman PMJ. Effect of dietary polyunsaturated fatty acids on reproductive output and larval growth of bivalves. J Exp Mar Biol Ecol 2003; 296: 199-213.
[21] Hochachka PW and Somero GN. Biochemical adaptation: mechanism and process in physiological evolution. New York: Oxford University Press; 2002.
[22] Miglioli A, Dumollard R, Balbi T, Besnardeau L and Canesi L. Characterization of the main steps in first shell formation in Mytilus galloprovincialis: possible role of tyrosinase. Proc Biol Sci 2019; 286: 20192043.
[23] Miglioli A, Balbi T, Besnardeau L, Dumollard R and Canesi L. Bisphenol A interferes with first shell formation and development of the serotoninergic system in early larval stages of Mytilus galloprovincialis. Sci Total Environ 2021; 758: 144003.
[24] Miglioli A, Balbi T, Montagna M, Dumollard R and Canesi L. Tetrabromobisphenol A acts a neurodevelopmental disruptor in early larval stages of Mytilus galloprovincialis. Sci Total Environ 2021; 793: 148596.
[25] Miglioli A. Pathways of endocrine disruption in the larval development of the mediterranean mussel Mytilus galloprovincialis. Gênes, Italie: Doctoral dissertation (Sorbonne Université, Università degli Studi di Genova); 2021.
[26] Balbi T, Franzellitti S, Fabbri R, Montagna M, Fabbri E and Canesi L. Impact of bisphenol A (BPA) on early embryo development in the marine mussel Mytilus galloprovincialis: effects on gene transcription. Environ Pollut 2016; 218: 996-1004.
[27] Folch J, Lees M and Sloane Stanley GH. A simple method for the isolation and purification of total lipides from animal tissues. J Biol Chem 1957; 226: 497-509.
[28] Novak M, Krpan T, Panevska A, Shewell LK, Day CJ, Jennings MP, Guella G and Sepčić K. Binding specificity of ostreolysin A6 towards Sf9 insect cell lipids. Biochim Biophys Acta Biomembr 2020; 1862: 183307.
[29] Gerdol M, Moreira R, Cruz F, Gómez-Garrido J, Vlasova A, Rosani U, Venier P, Naranjo-Ortiz MA, Murgarella M, Greco S, Balseiro P, Corvelo A, Frias L, Gut M, Gabaldón T, Pallavicini A, Canchaya C, Novoa B, Alioto TS, Posada D and Figueras A. Massive gene presence-absence variation shapes an open pan-genome in the Mediterranean mussel. Genome Biol 2020; 21: 275.
[30] Pang Z, Chong J, Zhou G, de Lima Morais DA, Chang L, Barrette M, Gauthier C, Jacques PE, Li S and Xia J. MetaboAnalyst 5.0: narrowing the gap between raw spectra and functional insights. Nucleic Acids Res 2021; 49: W388-W396.
[31] Lee HG, Joo M, Park JM, Kim MA, Mok J, Cho SH, Sohn YC and Lee H. Lipid profiling of Pacific abalone (Haliotis discus hannai) at different developmental stages using ultrahigh performance liquid chromatography-tandem mass spectrometry. J Anal Methods Chem 2022; 2022: 5822562.
[32] Gebai A, Gorelik A, Li Z, Illes K and Nagar B. Structural basis for the activation of acid ceramidase. Nat Commun 2018; 9: 1621.
[33] Leroy F, Meziane T, Riera P and Comtet T. Seasonal variations in maternal provisioning of Crepidula fornicata (Gastropoda): fatty acid composition of females, embryos and larvae. PLoS One 2013; 8: e75316.
[34] Soudant P, Marty Y, Moal J, Masski H and Samain JF. Fatty acid composition of polar lipid classes during larval development of scallop Pecten maximus (L.). Comp Biochem Physiol A 1998; 121: 279-288.
[35] Ramesh K, Melzner F, Griffith AW, Gobler CJ, Rouger C, Tasdemir D and Nehrke G. In vivo characterization of bivalve larval shells: a confocal Raman microscopy study. J R Soc Interface 2018; 15: 20170723.
[36] Liu Z, Zhang Y, Zhou Z, Zong Y, Zheng Y, Liu C, Kong N, Gao Q, Wang L and Song L. Metabolomic and transcriptomic profiling reveals the alteration of energy metabolism in oyster larvae during initial shell formation and under experimental ocean acidification. Sci Rep 2020; 10: 6111.
[37] Balbi T, Auguste M, Ciacci C and Canesi L. Immunological responses of marine bivalves to contaminant exposure: contribution of the -omics approach. Front Immunol 2021; 12: 618726.
[38] Bieberich E. There is more to a lipid than just being a fat: sphingolipid-guided differentiation of oligodendroglial lineage from embryonic stem cells. Neurochem Res 2011; 36: 1601-1611.
[39] Russo D, Parashuraman S and D'Angelo G. Glycosphingolipid-protein interaction in signal transduction. Int J Mol Sci 2016; 17: 1732.
[40] Dreier DA, Nouri MZ, Denslow ND and Martyniuk CJ. Lipidomics reveals multiple stressor effects (temperature × mitochondrial toxicant) in

the zebrafish embryo toxicity test. Chemosphere 2021; 264: 128472.
[41] Pauletto M, Milan M, de Sousa JT, Huvet A, Joaquim S, Matias D, Leitão A, Patarnello T and Bargelloni L. Insights into molecular features of Venerupis decussata oocytes: a microarray-based study. PLoS One 2014; 9: e113925.
[42] Eliyahu E, Park JH, Shtraizent N, He X and Schuchman EH. Acid ceramidase is a novel factor required for early embryo survival. FASEB J 2007; 21: 1403-1409.
[43] Riddle EL, Rau KS, Topham MK, Hanson GR and Fleckenstein AE. Ceramide-induced alterations in dopamine transporter function. Eur J Pharmacol 2003; 458: 31-36.
[44] Stiban J. Bioactive ceramides in health and disease. AEMB 1159 Stiban; 2019.
[45] Varre JV, Holland WL and Summers SA. You aren't IMMUNE to the ceramides that accumulate in cardiometabolic disease. Biochim Biophys Acta Mol Cell Biol Lipids 2022; 1867: 159125.
[46] Garrabou J, Gómez-Gras D, Ledoux JB, Linares C, Bensoussan N, López-Sendino P, Bazairi H, Espinosa F, Ramdani M, Grimes S, Benabdi M, Souissi JB, Soufi E, Khamassi F, Ghanem R, Ocaña O, Ramos-Esplà A, Izquierdo A, Anton I, Rubio-Portillo E, Barbera C, Cebrian E, Marbà N, Hendriks IE, Duarte CM, Deudero S, Díaz D, Vázquez-Luis M, Alvarez E, Hereu B, Kersting DK, Gori A, Viladrich N, Sartoretto S, Pairaud I, Ruitton S, Pergent G, Pergent-Martini C, Rouanet E, Teixidó N, Gattuso JP, Fraschetti S, Rivetti I, Azzurro E, Cerrano C, Ponti M, Turicchia E, Bavestrello G, Cattaneo-Vietti R, Bo M, Bertolino M, Montefalcone M, Chimienti G, Grech D, Rilov G, Tuney Kizilkaya I, Kizilkaya Z, Eda Topçu N, Gerovasileiou V, Sini M, Bakran-Petricioli T, Kipson S and Harmelin JG. Collaborative database to track mass mortality events in the mediterranean sea. Front Mar Sci 2019; 6: 707.
[47] Wijsman JWM, Troost K, Fang J and Roncarati A. Global production of marine bivalves. Trends and challenges. In: Smaal AC, editors. Goods and Services of Marine Bivalves. Cham; 2019.
[48] Avdelas L, Avdic-Mravlje E, Borges Marques AC, Cano S, Capelle JJ, Carvalho N, Cozzolino M, Dennis J, Ellis T, Fernández Polanco JM, Guillen J, Lasner T, Le Bihan V, Llorente I, Mol A, Nicheva S, Nielsen R, Oostenbrugge H, Villasante S, Visnic S, Zhelev K and Asche F. The decline of mussel aquaculture in the European Union: causes, economic impacts and opportunities. Rev Aquacult 2021; 13: 91-118.

Table S1. Primers sequences for qPCR

	Gene	Primers	Amplicon size bp	Amplification efficiency (%)
Ceramide metabolism	*SP2*	Fwd: TTT GGT GCT GCT GGT GGT TA Rev: ACT GCG GGA CAC ATT GTA GG	104	103
	KDSR2	Fwd: TCA AGT GGC ATA GGG AAG GC Rev: CAA CCT TTG CAG CTT CGA GT	103	98
	GC2	Fwd: TGT TGG AGT TGA CCC TCA CC Rev: TGC TGA ATC CAT TTC ATC TTG GA	106	98
	aCDase	Fwd: CGA TTA TGG GAG GGG TTC GC Rev: CCA TCT TCC TGA CTT GGC GT	101	103
Housekeeping genes	*EF-α1*	Fwd: CGT TTT GCT GTC CGA GAC ATG Rev: CCA CGC CTC ACA TCA TTT CTT G	135	99
	HEL	Fwd: GCA CTC ATC AGA AGA AGG TGG C Rev: GCT CTC ACT TGT GAA GGG TGA C	129	132

SP2 = serine palmitoyltransferase-1; KDSR2 = 1,3-ketodihydrosphingosine reductase; GC2 = ceramide glucosyltransferase; aCDase = acid ceramidase; EF-α1 = Elongation factor-α1; HEL = Helicase.

A

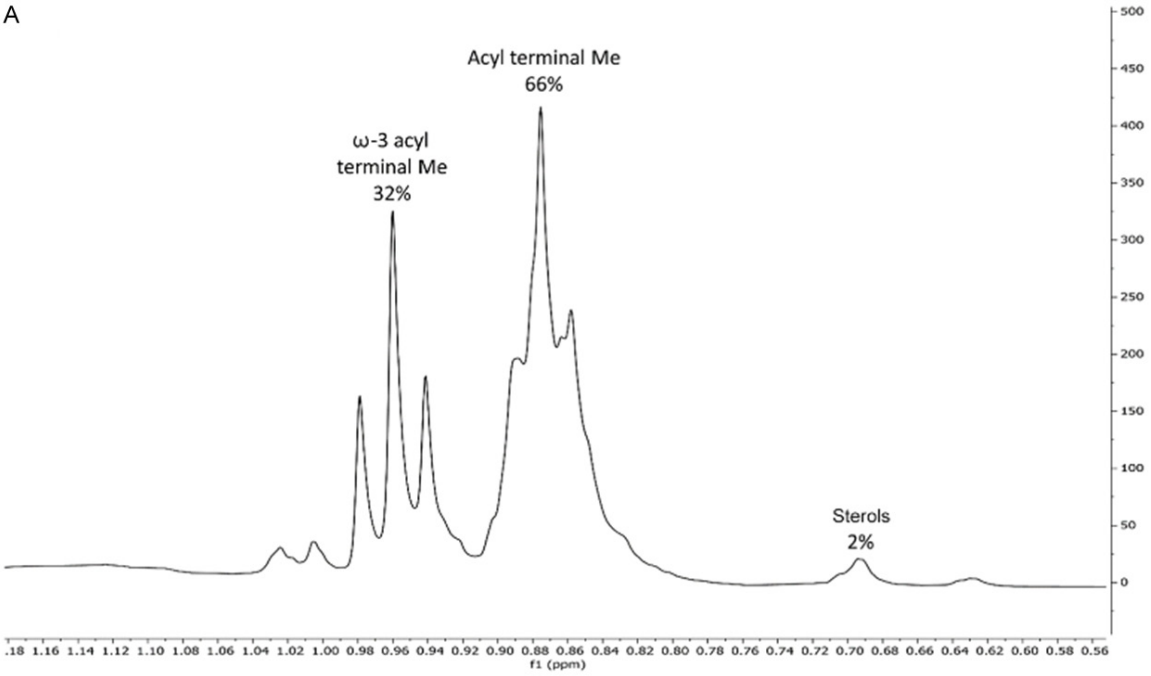

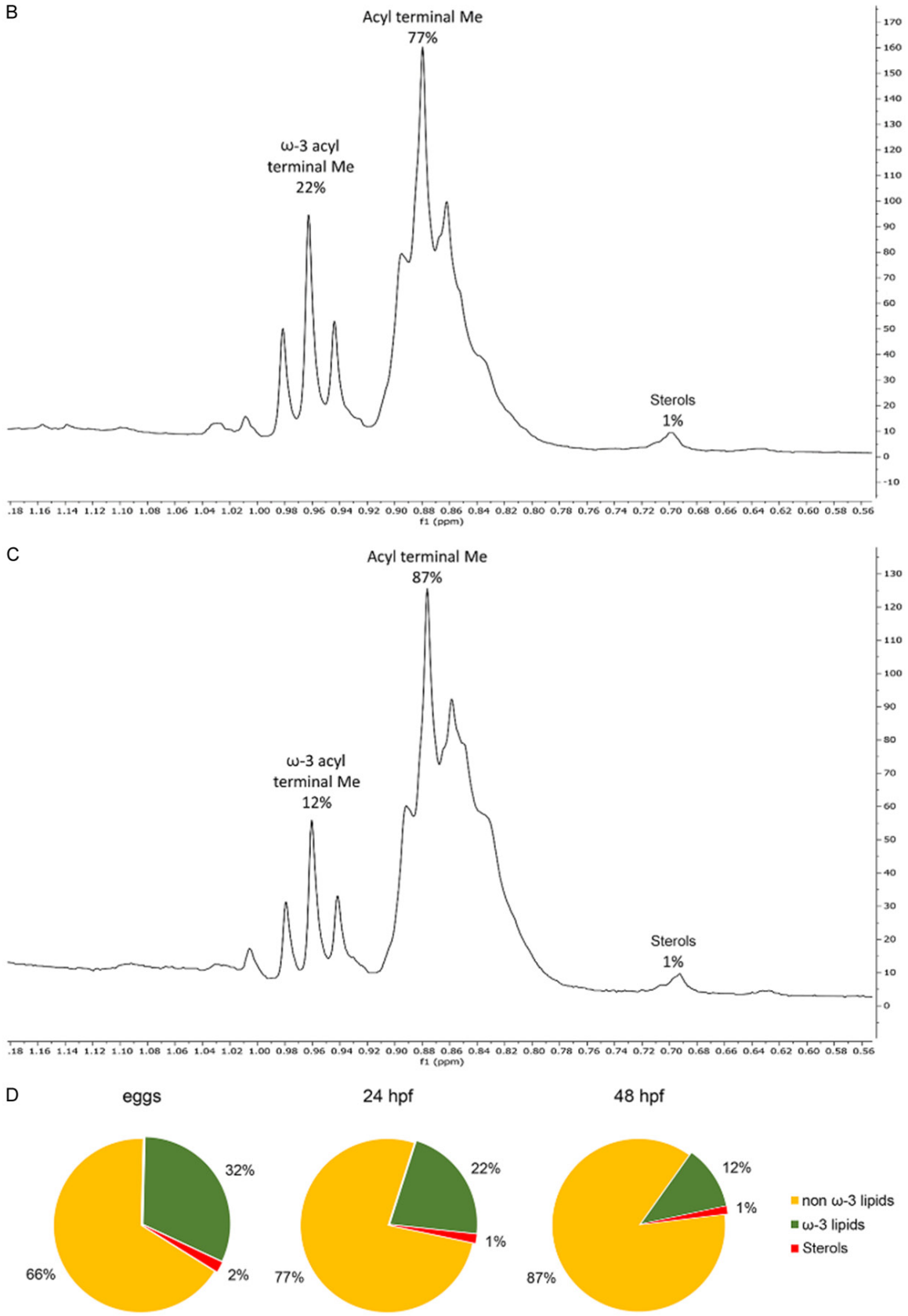

Figure S1. ^{1}H-NMR spectra of total lipid extracts from *M. galloprovincialis* eggs (A) and larvae at 24 hpf (B) and 48 hpf (C). Signals shown are relative to acyl chain terminal methyl of ω-3 and non ω-3 lipids, and to the angular methyl

of free sterols. Molar fraction is calculated by integration of these three signals and expressed as percentage over their integral sum. (D) Data are reported as relative composition (% values) of non ω-3 lipids, ω-3 lipids and total sterols in eggs and larvae at 24 and 48 hpf.

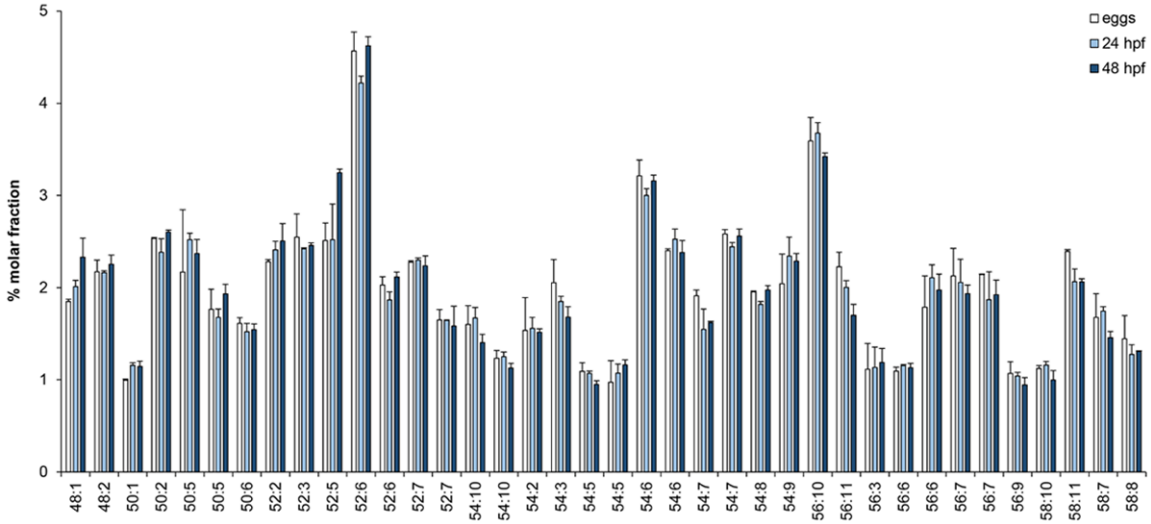

Figure S2. LC-MS analysis of main triglycerides (TAG) species (1% cutoff) in lipid extracts from *M. galloprovincialis* eggs and larvae at 24 and 48 hpf. Data, representing the mean ± stdev of 3 samples, are expressed as % molar ratio of total TAG.

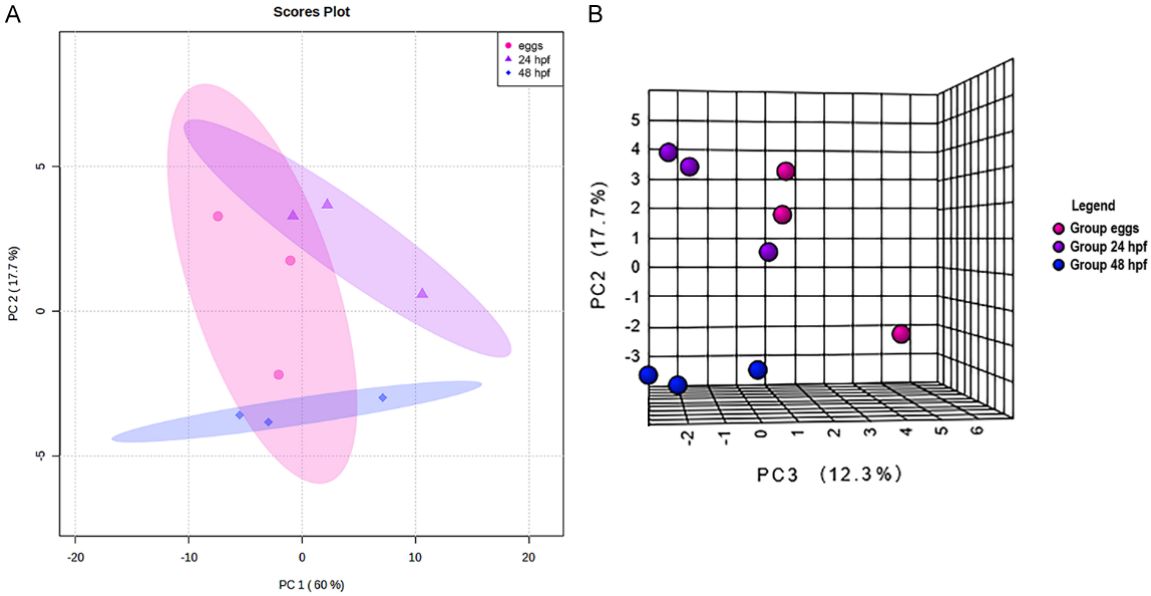

Figure S3. PCA score plots of phospholipid data (PC, PE, PI, CAEP species) in the three groups (eggs, 24 and 48 hpf larvae). The explained variances are shown in brackets. A. 2D plot of Principal Components 1 and 2. The colored ellipses represent the 95% confidence interval, and the explained variations are shown in brackets. B. 3D plot of Principal Components 2 and 3.

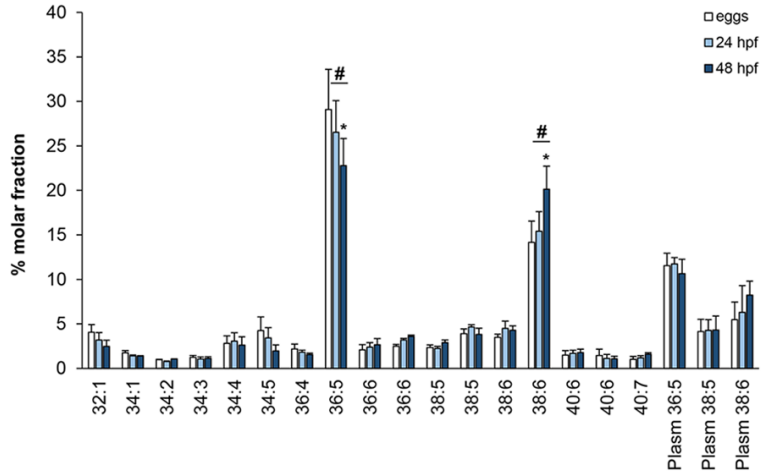

Figure S4. LC-MS analysis of main PC species in lipid extracts from *M. galloprovincialis* eggs and larvae at 24 and 48 hpf. Data, representing the mean ± stdev of 3 samples, are expressed as % molar ratio of total PC. Significant differences are reported (* eggs *vs* 24 or 48 hpf; # 24 *vs* 48 hpf; P≤0.05, Two-way ANOVA, Bonferroni post-test).

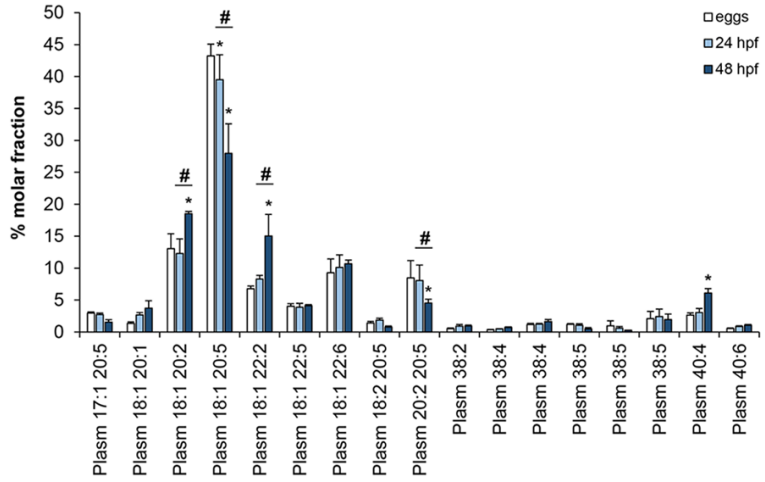

Figure S5. LC-MS analysis of main pPE species in lipid extracts from *M. galloprovincialis* eggs and larvae at 24 and 48 hpf. Data, representing the mean ± stdev of 3 samples, are expressed as % molar ratio of total plasmenyl-PE. Significant differences (* eggs *vs* 48 hpf; # 24 *vs* 48 hpf; P≤0.05, Two-way ANOVA, Bonferroni post-test) are reported.

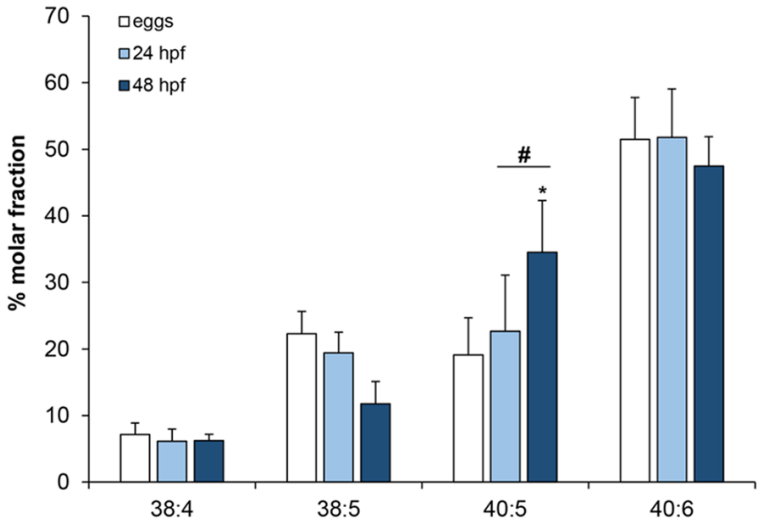

Figure S6. LC-MS analysis of main PI species in lipid extracts from *M. galloprovincialis* eggs and larvae at 24 and 48 hpf. Data, representing the mean ± stdev of 3 samples, are expressed as % molar ratio of total PI. Significant differences (* eggs vs 48 hpf; # 24 vs 48 hpf; P≤0.05, Two-way ANOVA, Bonferroni post-test) are reported.